RESEARCH ARTICLE

TECHNIQUES AND RESOURCES

4D atlas of the mouse embryo for precise morphological staging

Michael D. Wong[1,2,*], Matthijs C. van Eede[1], Shoshana Spring[1], Stefan Jevtic[1], Julia C. Boughner[3], Jason P. Lerch[1,2] and R. Mark Henkelman[1,2]

ABSTRACT

After more than a century of research, the mouse remains the gold-standard model system, for it recapitulates human development and disease and is quickly and highly tractable to genetic manipulations. Fundamental to the power and success of using a mouse model is the ability to stage embryonic mouse development accurately. Past staging systems were limited by the technologies of the day, such that only surface features, visible with a light microscope, could be recognized and used to define stages. With the advent of high-throughput 3D imaging tools that capture embryo morphology in microscopic detail, we now present the first 4D atlas staging system for mouse embryonic development using optical projection tomography and image registration methods. By tracking 3D trajectories of every anatomical point in the mouse embryo from E11.5 to E14.0, we established the first 4D atlas compiled from *ex vivo* 3D mouse embryo reference images. The resulting 4D atlas comprises 51 interpolated 3D images in this gestational range, resulting in a temporal resolution of 72 min. From this 4D atlas, any mouse embryo image can be subsequently compared and staged at the global, voxel and/or structural level. Assigning an embryonic stage to each point in anatomy allows for unprecedented quantitative analysis of developmental asynchrony among different anatomical structures in the same mouse embryo. This comprehensive developmental data set offers developmental biologists a new, powerful staging system that can identify and compare differences in developmental timing in wild-type embryos and shows promise for localizing deviations in mutant development.

KEY WORDS: OPT, Embryo, 3D, 4D, Imaging, Development, Staging

INTRODUCTION

The accurate and precise developmental staging of embryos is required for progress within developmental biology. For instance, determining the stage of an embryo's development is necessary for comparing embryonic development within and among groups. Unlike zebrafish, for which prenatal development can be observed continuously, mouse development can only be studied by interrupting it at static time points; thus, staging mouse embryos has for decades suffered because of this discontinuity of data. Numerous staging systems for mouse embryonic development based on parameters such as gestational age, global size, and anatomical landmarks have been proposed in an attempt to assign a discrete developmental scale (Michos et al., 2004; Theiler, 1972). These staging systems are simplistic and thus do not capture the

complex remodeling and growth that occurs in internal anatomical structures and, consequently, cannot stage embryonic mice comprehensively, at high granularity. Our work addresses this imprecision in staging by using the wealth of additional information provided by high-resolution 3D imaging to develop a staging system that captures anatomical development at the structural level.

The age of an embryo is typically defined as the number of days post coitum (dpc), but this definition is not an accurate indicator of anatomical stage. In mice, breeding is typically set up in the late afternoon and the morning that a vaginal plug is detected is defined as 0.5 dpc at noon. Thus, time of conception is uncertain, resulting in an expected inter-litter variation of development of up to 12 hours. In addition, mouse embryo littermates harvested at the same time are often at different developmental stages as a result of variable implantation time and nutrient disparity (Pang et al., 2014; Papaioannou and Behringer, 2005). Owing to the observed variability in development of age-matched mouse embryos, staging systems based on anatomical structure and gross size have been developed.
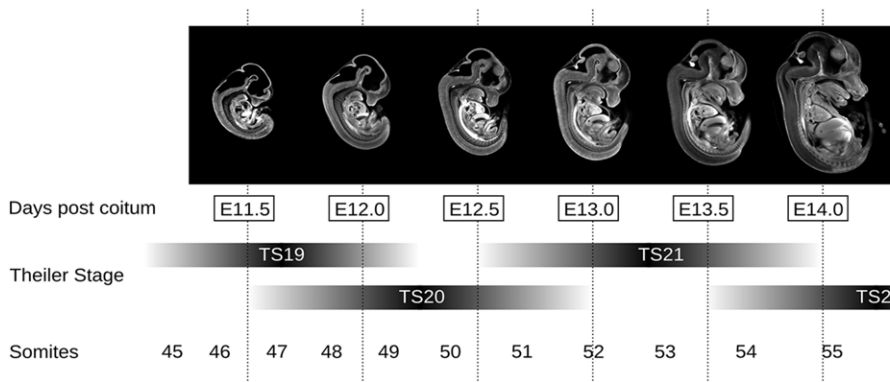
Theiler staging is a classical staging system that scales mouse embryo development by observable morphological features that can be visualized through a dissection microscope (Theiler, 1972). These features include the earliest sign of digits [Theiler stage (TS) 20] and the indentation of the anterior footplate (TS 21). Most Theiler stages include multiple definitions of features of organ systems, including the limbs, eyes, whiskers, and epidermis. Because these annotations are qualitative, individual researchers may interpret and subsequently apply the Theiler staging system differently.

Somites begin to appear at embryonic day (E) 7.5 and increase to a final total of 60 somites at E14.0 before forming the vertebrae and other mesoderm-derived tissues. Somite number is predominantly used for embryo staging between E8.0 and E10.5 because there is an increase of 22 somites in that span and somites are clearly visible to allow for reliable counts using a dissection microscope (Michos et al., 2004). Somite staging is particularly useful for early cardiovascular development because the essential events in the development of the early heart and vasculature occur within these time points (Walls et al., 2008).

Both Theiler and somite staging suffer because the lengths of their stages vary in terms of dpc (Fig. 1). This is a problem, especially late in gestation, as the number of stages begins to decrease per day to the point at which developmental events in organogenesis occur much faster than the temporal sampling of Theiler's stages. Also, both staging systems assume that development throughout the whole mouse embryo is perfectly synchronous and accurately reflected by a limited number of feature landmarks. A previous study showed that the right and left limb buds of the same embryo can form with significant asynchronicity (Boehm et al., 2011); therefore, cardiovascular, lung, renal and liver development are probably also asynchronous with somite number and/or the organ systems that define Theiler staging.

[1]Mouse Imaging Centre, Hospital for Sick Children, Toronto, Ontario, M5T 3H7, Canada. [2]Department of Medical Biophysics, University of Toronto, Toronto, Ontario, M5G 1L7, Canada. [3]Department of Anatomy and Cell Biology, University of Saskatchewan, Saskatoon, Saskatchewan, S7N 5E5, Canada.

*Author for correspondence (mwong@mouseimaging.ca)

Fig. 1. Classical staging systems spanning E11.5 to E14.0. Mid-sagittal sections of OPT mouse embryo images are positioned along the staging time line of three different staging systems: days post coitum (dpc), Theiler staging, and somite number. The temporal sampling of Theiler staging is in the order of 1.5-2 dpc during mid-gestation, and the anatomical landmark approach causes overlap in its stage definitions. By mid-gestation, the formation rate of somites markedly decelerates, restricting the practical application of counting somites to stages E8.0-E11.5.

A staging system that is continuous throughout embryo development would be more precise than staging systems that sample discrete stages to define specific annotations like Theiler staging. A continuous staging system that incorporates normal variation in developmental day and stage would require a quantifiable biological process that could be measured and interpolated with gestational time. This concept was first employed for staging limb bud development in the mouse embryo by James Sharpe's group (Boehm et al., 2011), which accurately characterized the outline of the developing hind limb by smooth curves evolving in time. Based on curvature, they then developed an interpolated limb bud atlas that staged any subsequent mouse embryo limb bud with a simple curvature measurement fitted to their reference atlas.

Here, we describe a continuous staging system over the whole mouse embryo volume made possible with high-resolution 3D optical projection tomography (OPT) images (Sharpe et al., 2002; Wong et al., 2013). For this paper, 3D images were acquired at six developmental time points spaced at 12-h intervals between E11.5 and E14.0. Homologous points in anatomy were tracked using image registration (Collins and Evans, 1997; Walls et al., 2008) and the resulting displacement vectors were fitted to cubic splines over developmental time (the fourth dimension) and interpolated. The result was a four-dimensional (4D) developmental atlas of 3D whole embryo volume image data over gestational time to which any subsequent mouse embryo 3D image data can be compared and staged. With the development and growth of every organ system interpolated in time, the development of these systems is accurately described even if it is asynchronous. Organs such as the heart, brain,

lung and liver can also each be individually staged based on this reference 4D developmental atlas. Because each individual point in anatomy, or voxel in the 3D image, is interpolated in 3D space over time, staging each voxel is possible resulting in a novel staging system with both high spatial and temporal resolution.

RESULTS

Generation of image models for the first iteration of the 4D atlas

The true mouse embryo morphology for any extraction time point (dpc) does not and cannot exist because of the ambiguity of the definition. We decided to calculate the mean morphology at a given developmental time as the model for that time point. Specifically, for each of the six developmental time points imaged, a population average image of the eight randomly selected mouse embryo images was generated through group-wise image registration (Fig. 2). Therefore, the six population average images acted as models of 3D morphology at their corresponding extraction time points for the first iteration of cubic spline interpolation. This first set of six model images separated by half-day intervals was the first iteration of the 4D atlas.

Second iteration of the 4D atlas: cubic spline fitting of morphological development

To track each homologous point in anatomy across the six time points, the six mouse embryo model images of the first iteration of the 4D atlas were subjected to another round of image registration. Here, each of these model images was registered to its adjacent time point, using source-to-target registration, in the order of increasing
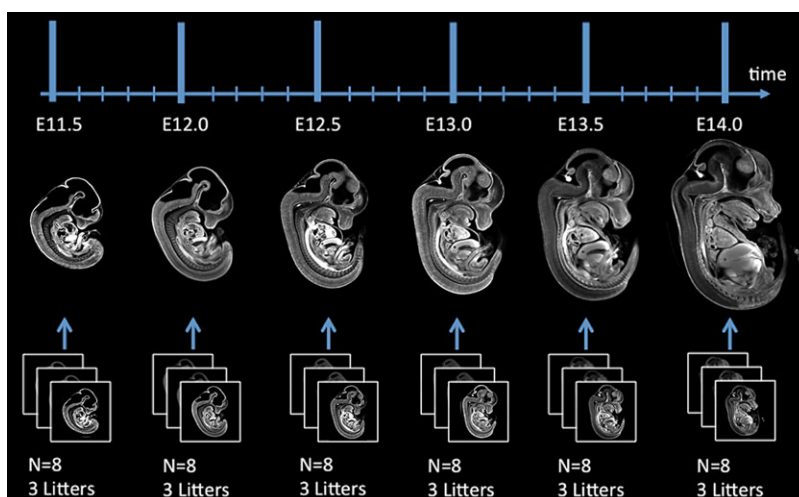
Fig. 2. Generation of the image models for the six extraction time points. Eight mouse embryo OPT 3D images were registered into a population average model image at each extraction time point.

time. Anatomical differences due to organ growth and subtle changes in structural shape could be registered between two gestational stages. However, organogenesis and tissue remodeling that occurs rapidly between E11.5 and E14.0 prevented successful image registration between embryo images differing by more than half a day due to insufficient anatomical homology (data not shown). Therefore, it was essential to register the model images to adjacent time points at half-day intervals in order to maximize anatomical homology between time points. This second round of image registration generated five displacement vectors that described in 3D space the position of every homologous point of anatomy at all six time points (Fig. 3).

Rather than the linear displacements shown in Fig. 3, each point in anatomy traverses along curves in 3D space. Therefore, for every homologous image voxel, the five displacement vectors were fitted to a 3D cubic B-spline over time. In the first iteration of the 4D atlas, the six model population average images were set as true data points; therefore, the spline fit was weighted such that the spline was forced to pass through each of the vector components. The spline function can be evaluated at any intermediate time point to calculate the displacement vector that describes the position of each voxel at any time point. These splines can also be used to generate an interpolated 3D image for any arbitrary time point by applying the transformation to the mouse embryo model image closest in age (dpc). For this second iteration of the 4D atlas, 3D mouse embryo images were generated using the fitted splines for every 0.1 dpc between E11.5 and E14.0, totaling 26 entries for this atlas.

Re-timestamping the initial data set for internal consistency

The six model images in the first iteration of the 4D atlas were composed of an average of eight individual mouse embryo images for each time point. These individual embryo images were close to the composite average embryo image used to define the first iteration 4D atlas, but not exactly at identical stages of development. To stage each of these forty-eight embryos using the second iteration of the 4D atlas, each embryo image was independently re-registered to each of the 26 interpolated 3D embryo images, plus four additional extrapolated images (E11.3, E11.4, E14.1, E14.2) using a six-parameter, rigid registration. The rigid registration aligned the position and orientation of the source embryo images with the interpolated embryo images from the 4D atlas. Staging was performed by identifying which 4D atlas image had the maximum normalized cross correlation with the source image. The corresponding time point of this 4D atlas image was denoted the re-timestamped stage of the source embryo image replacing its initial time corresponding to its age of extraction. The additional four extrapolated images (E11.3, E11.4, E14.1, E14.2) were included in order to observe a clear maximum normalized cross correlation at the E11.5 and E14.0 time point. The

re-timestamped stage, in embryonic days, of each of the input mouse embryo images is presented in Fig. 4. Mouse embryos that were staged younger than E11.5 and older than E14.0 are not shown ($n=5$) because data, or model images, were not obtained outside of this time window.

The apparent embryonic stage for mouse embryos harvested at the same time (dpc) can be as much as half a day on either side of the nominal time. In addition, mouse embryos harvested at two different time points separated by half a day (E11.5-E12.0, E12.5-E13.0) can be at the same developmental stage. It is also noteworthy that because the mouse embryos were chosen at random from three different litters, the distribution of embryo development about the mean differed among the six extraction time points.

### Third iteration of the 4D atlas: more accurate image models

From the second iteration of the 4D atlas, approximate stages (dpc) were determined for each mouse embryo in the nominal set. A third iteration of the 4D atlas was fine-tuned using model images from source embryo images with re-timestamped ages. For each of 26 stages separated into 0.1 dpc intervals, we performed a group-wise registration using the source images that were re-timestamped during the second iteration of the 4D atlas. This group-wise registration was weighted, such that embryo images that were staged closer to the time point in question had more influence on the generated population average image. For example, the group-wise registration that generated an E12.0 model average image included embryos staged within a range of ±0.2 dpc about the E12.0 time point. Gaussain weighted ($\sigma=0.08$ dpc) group-wise registration was performed by weighting the transforms of the pair-wise affine registration and then applying the weights to the image intensities of each corresponding embryo image when generating population average images for each non-linear iteration. The integral weight was scaled to 100%.

Once population average images were generated for each of the 26 time points, source-to-target image registrations were performed between adjacent time points in the direction of increasing time. These displacement vectors for every image voxel were generated and a cubic spline was fitted to the x, y and z components over the 26 time points. For this iteration, the spline fit was not forced to pass through the 26 gestational time points, allowing for less flexibility when interpolating time and space. The splines were then used to generate interpolated 3D images at every 0.05 dpc over the same gestational range (E11.5-E14.0) to produce a total of 51 stages of embryo development. This third iteration of the 4D atlas doubles the temporal sampling of the second iteration yielding a temporal resolution equivalent to 72 min (Movie 1, Fig. S1). All 51 interpolated images of the 4D atlas are open source and available at: http://www.mouseimaging.ca/technologies/mouse_atlas/4D_atlas_mouse_embryo.html.
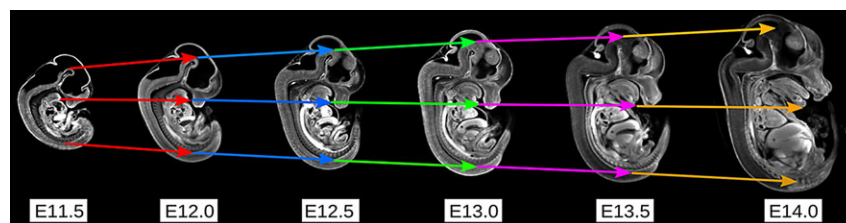
Fig. 3. Tracking homologous points in anatomy through development using image registration. Each mouse model image was registered to the next image at the adjacent time point. This registration process generated displacement vectors to describe the position of each point in anatomy at a given time point. The colors of each vector represent displacement vectors between adjacent time points, vectors that were generated through the image registration of model images between the time points. Three sets of displacements through homologous points are shown.
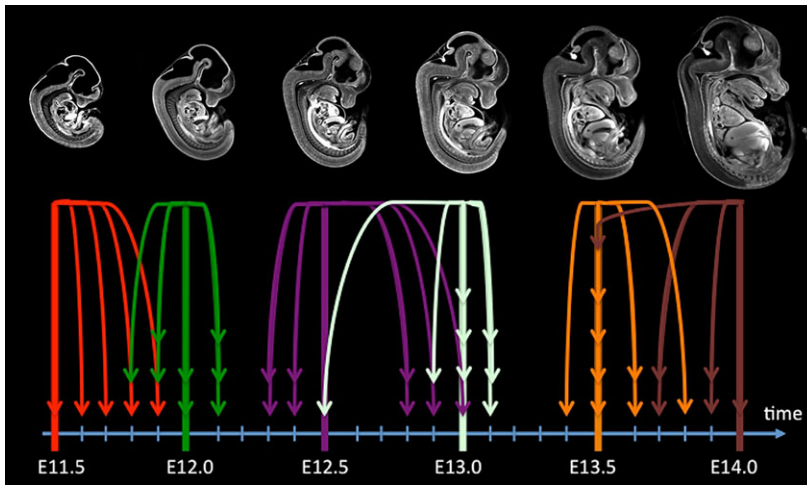
Fig. 4. Re-timestamping the initial set of images according to the second iteration of the 4D atlas. This schematic shows the evaluated stage of each of the mouse embryos in the original set. Embryos that were staged either older than E14.0 or younger than E11.5 are not shown (n=5). Arrow color indicates embryos extracted on the same dpc. The stage of mouse embryos harvested at a given dpc can deviate by as much as 0.5 dpc from the mean. The calculated average standard deviation of the staged mouse embryos about the six extraction time points is 0.17 dpc.

As an illustration of the information contained in the 4D atlas, we present (in Fig. 5) several slices showing heart development over three time points. Non-stereotype patterning, such as the development of cardiac trabeculation, is blurred out in the 4D average, but is clearly evident in the equivalent slice from a single individual (Fig. 5D) that contributes to the atlas.

Performing several iterations of cubic spline fitting and re-timestamping of the same 48 source mouse embryo images converged to a self-consistent 4D atlas data set. Re-timestamping the initial data set using a third iteration of the 4D atlas revealed that the evaluated stage of each of the input embryos images remained consistent between the second and third atlas iterations. Of the 43 original mouse embryo images that were staged from E11.5 to E14.0, 97% drifted in stage by no more than 0.1 dpc between the second and third 4D atlas iterations. The largest discrepancy (n=1) was 0.15 dpc or the equivalent of 2 h gestation time. Thus, we conclude that a fourth iteration of the 4D atlas was not required because the observed accuracy of 0.15 dpc is finer than the granularity of any other existing metric used to define murine embryonic development, including the limb-morphometic staging system (Boehm et al., 2011).

Computer-automated staging at the global, structural and voxel level

We next investigated whether staging mouse embryos using the described 4D atlas could be computer automated. For this test, a 3D OPT image data set of the mouse embryo was required that was within the range of developmental stages (E11.5-E14.0) of the 4D atlas. All 51 mouse embryo images (one image per 0.05 dpc) in the third and final iteration of the 4D atlas were registered in turn to the test mouse embryo image to be staged.

As opposed to a group-wise registration, the pair-wise affine registration was replaced by individual source-to-target affine registrations towards the sample image. In addition, the population average images that act as the target image in each nonlinear iteration were replaced by the sample image as well. To stage the mouse embryo image globally, the normalized cross correlation was calculated between the sample embryo and each embryo image in the 4D atlas subsequent to the six-parameter, rigid registration. As previously described, we define the global embryonic stage as the time point that corresponds to the 4D atlas mouse embryo image with the highest normalized cross correlation with the sample embryo.

For example, a wild-type mouse embryo that was part of the initial data set and extracted at 12.5 dpc was staged using our described automated staging pipeline. Post-rigid image registration, the normalized cross correlation value between this test mouse embryo and each image in the 4D atlas was at its maximum value at E12.80 (Fig. 6). The red contours correspond to intensity gradients (anatomical boundaries) in the sample embryo image and are superimposed onto five of the 4D atlas images. The red contours most visually corresponded to the image intensities displayed in the E12.80 image, further validating the use of the normalized cross
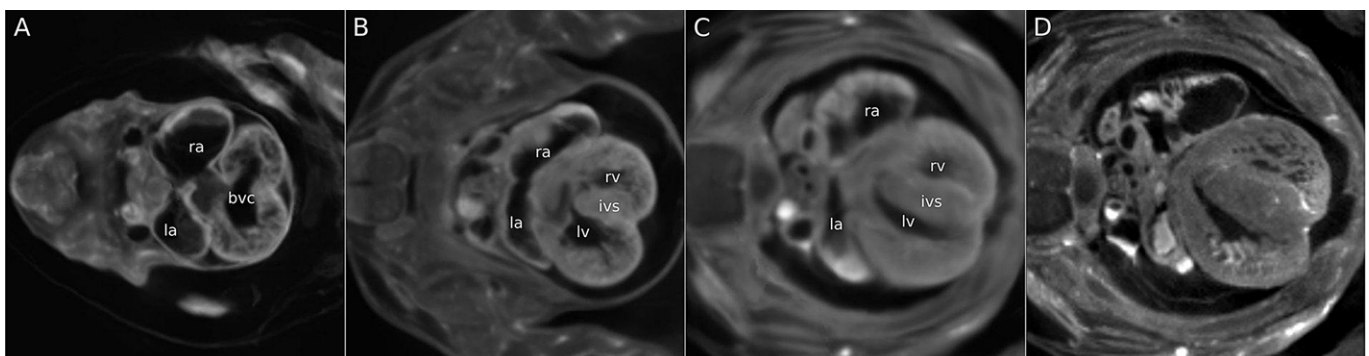
Fig. 5. Visualizing heart developmental events using the 4D atlas. (A-D) From the 4D atlas, three slices showing average heart development at E11.50 (A), E12.75 (B) and E13.70 (C) are shown. Formation of the chambers (la, left atrium; lv, left ventricle; ra, right atrium; rv, right ventricle) is clearly visible. The bulbar ventricular canal (bvc), which is open at E11.50 (A), is becoming closed by the interventricular septum (ivs) at E12.75 (B) and is fully closed at E13.70 (C). Cardiac trabeculation, which does not follow stereotypical patterning, is blurred out in the average image (C), but is evident in the equivalent slice of any single individual embryo at E13.70 (D).
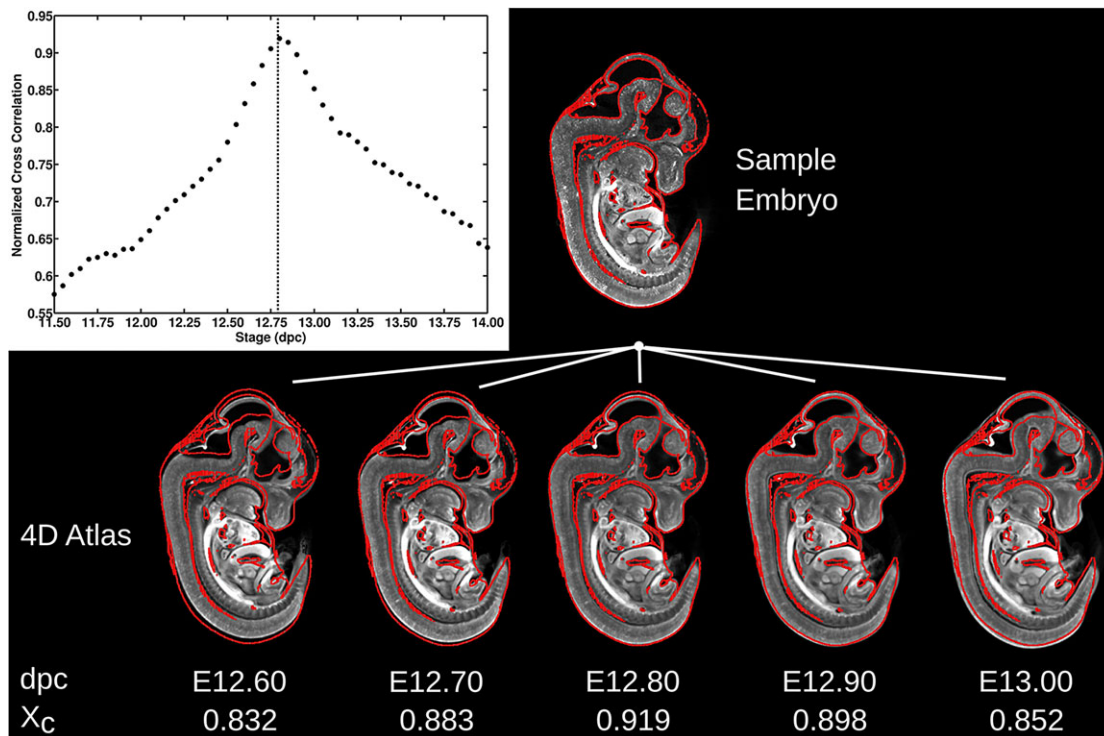
Fig. 6. Global staging using normalized cross correlation. A plot of the calculated normalized cross correlation between a sample embryo and the 51 mouse embryo images and their corresponding stages in the 4D atlas illustrates a global maximum of 12.80 dpc. In the images, the red contours outline the edges of the sample embryo and are superimposed onto five mouse embryos of the 4D atlas that were rigidly registered to the sample embryo. The normalized cross correlation (X_c) is highest with the E12.80 mouse embryo and the red contours fit best with that image as well. It is of note that X_c is calculated over the whole 3D volume and not only this 2D section.

correlation as a staging measure for the similarity between mouse embryo images. Staging by this method determines the average stage over the whole mouse embryo volume and does not account for asynchrony in development of individual organ systems.

Asynchronicity was investigated by assigning an embryonic stage for every anatomical point in 3D space. The stage of each point in anatomy was calculated by determining which 4D atlas image required the minimum displacement to align with the test image, per voxel. The magnitude of each displacement vector at every voxel in the test image was calculated from the deformation fields produced for each 4D atlas image to register with the test image. The displacement magnitudes for each voxel are fitted to a second-order polynomial over time (dpc) as described by the 4D atlas. We define the time component of the vertex of this quadratic fit as the stage for that image voxel and its corresponding point in anatomy. The calculated vertex of the second-order polynomial fit is not confined to the 0.05 dpc sampling of the 4D atlas, such that the stage for each image voxel can have a value of any arbitrary precision. A new staging 3D data set was produced for which the evaluated stage of each voxel is mapped to its corresponding location in the test mouse embryo image space. Superimposing the staging 3D data set onto the intensity image of the test mouse embryo presents a developmental stage for every point in anatomy.

The stage of each voxel for the test mouse embryo example was calculated and presented as a heat map of gestational age superimposed on its corresponding intensity image (Fig. 7A,B). The embryonic stage of the embryo over the whole volume appeared to be consistent at the voxel level ($\sim$E12.80) when using the total gestational range of the 4D atlas as the lower and upper bounds of the color map scale bar (Fig. 7A). Differential staging of individual organs is better illustrated by restricting the color scale to a developmental range of $\pm$0.5 dpc around the calculated global stage of E12.80 (Fig. 7B). As shown in Fig. 7B, the majority of the mouse embryo volume was staged at 12.80 dpc; however, several anatomical structures showed developmental asynchrony. For example, the dorsal surface and the right atrium of the heart were staged a few hours younger at approximately 12.60 and 12.40 dpc, respectively.

The spatial resolution of this computed 3D staging data set is much higher than required for most applications in developmental biology. The ability to stage individual whole organs at the structural level is more valuable than analyzing the stages of each of the thousands of voxels within those structures. A 3D segmented atlas of individual organs, such as the one previously described in *Development* (Wong et al., 2012), can be used to calculate the average stage over all the voxels in the segmented structure of interest. Unfortunately, the 3D segmented atlas previously described (E15.5) cannot be used for the time points within the 4D atlas (E11.5-E14.0). Therefore, to illustrate this concept we have created a limited 4D segmented atlas in which the heart, liver, lung and brain ventricles were manually segmented. The preliminary segmented atlas resampled into the sample wild-type mouse embryo image space is visualized in 3D and in 2D in Fig. 7C,D. The heart, liver, lung and brain ventricles were staged by calculating the average stage of the voxels within the corresponding segmented regions (Fig. 7E). In this case, the evaluated stages of the heart, liver, lung and brain ventricles were 12.75±0.15, 12.83±0.09, 12.69±0.05 and 12.89±0.04 dpc, respectively (mean±s.d. of voxels in the segmented volume).

To demonstrate that developmental asynchrony is unique to each embryo, the staging pipeline was performed on a different wild-type mouse embryo that was harvested at E12.5, but was not
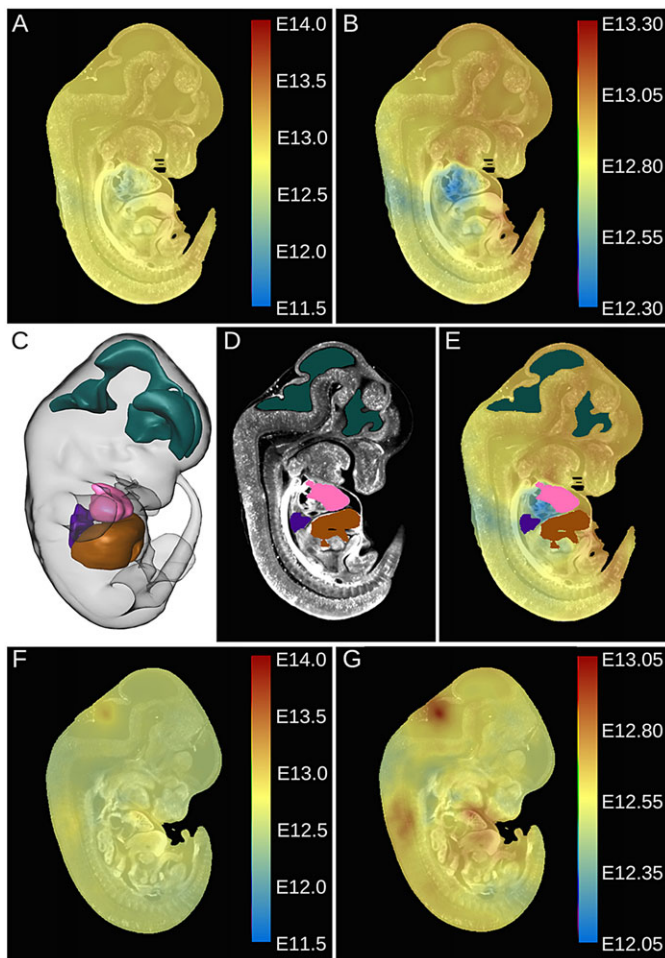
Fig. 7. Staging by voxel and by structure. (A,B) Voxel-wise staging is displayed for a mid-sagittal section of an embryo from the nominal set that was staged globally at E12.8. Broad (A) and tighter (B) color bar time scales are used to show the relative consistency of the staging over the volume and the asynchrony of development, respectively. (C-E) A limited segmented atlas of the heart (pink), liver (brown), lung (dark blue) and brain ventricles (aqua) is shown in 3D (C) and in 2D (D). The application of the segmented labels to measure the average stage for those regions is visually presented in E. (F,G) Voxel-wise staging is displayed for a mid-sagittal section of an additional embryo (not used to construct the 4D atlas) that was staged globally at E12.55.

part of the nominal data set of 48. The calculated global stage of this mouse embryo was 12.55 dpc and the per voxel staging is presented in Fig. 7F,G. Again, when using the time window of the 4D atlas as the bounds of the staging color bar (Fig. 7F) the embryonic stage appears consistent over the whole mouse embryo volume (~E12.55). However, using a developmental time window that is ±0.5 dpc about the global stage of E12.55 (Fig. 7G) revealed that areas in the dorsal cerebral aqueduct and ventral parts of the heart and liver are a few hours older than the calculated global stage. Using the segmented regions of the heart, liver, lung and brain ventricles, each was staged at the structural level as 12.66±0.09, 12.66±0.12, 12.60±0.03 and 12.60±0.12 dpc, respectively.

Even when primary embryo image data is not obtained from 3D OPT images, the 4D atlas can be used as a visual comparator to provide a view of average developmental anatomy and stage as shown in Fig. 8. In the future, computer algorithms that take into account the differing contrasts in Hematoxylin and Eosin staining compared with autofluorescence may be developed for finding such

correspondences. In the interim, visual comparison allows for staging precision of approximately ±0.1 dpc.

DISCUSSION
Development of a novel staging system
The generation of the 4D mouse embryonic developmental atlas and the computer-automated staging process described here is proof of principle that 3D morphology can be used to precisely measure the developmental stage of a given mouse embryo. Intuitively, the global staging system, using the normalized cross correlation of OPT images more accurately and comprehensively described the anatomical development of an embryo than do classical measures such as crown-to-rump length and body weight. Both crown-to-rump length and body weight characterize only one outer dimension of the mouse embryo volume. Unlike these global metrics, the normalized cross correlation summarizes the similarity in image intensities at each voxel between two images. Each point in anatomy described by each image voxel has equal weight and, therefore, the normalized cross correlation is a staging parameter that sums up the whole embryo anatomy.

This 4D staging system provides an unprecedented level of spatial and temporal resolution: evaluating an embryo's progression through development at the image voxel level results in ~10^9 individual staging measurements over the embryo volume. Based on the displacement vectors from the 4D atlas images to the sample image, these individual voxel measurements result in a smooth distribution of stage time points over the 3D volume (Fig. 7A,B,F,G). The 3D staging heat map is visually striking and thus clearly and quickly communicates even subtle asynchrony in development and growth among and within organ systems. The temporal sampling provided by the 4D atlas is fine enough to resolve developmental asynchrony of 0.05 dpc or the equivalent of 72 min.

In this regard, the resultant 3D staging data set can be segmented into individual organs to determine the embryonic state at the structural level. For this proof-of-principle study, the heart, liver, lung and brain ventricles were segmented for every time point in the 4D atlas. Classical staging techniques have been restricted to anatomical landmarks that can be observed exclusively on the surface of the embryo volume. The staging technique presented here also stages internal anatomy using quantifiable and unbiased metrics. Developmental biologists studying different systems, such as the developing heart, liver, brain, kidney and lung, can use this staging system equivalently.

The 4D mouse embryo atlas is not merely a reference baseline for the staging system, but can be used to investigate developmental trajectories of every observable anatomy with time. The 4D atlas can be visualized as a spatial 3D movie along the time axis to demonstrate the growth rate, 3D formation and morphogenesis of each organ. It is difficult, if not impossible, to display the richness and dynamics of the 4D atlas using 2D sections (Fig. S1). Only the mid-sagittal section of the 4D atlas is presented in each figure because any section other than the central slice will show anatomical structures traversing through it over time, making it difficult to track the homologous points in anatomy with development.

Re-timestamping the original data set according to the second iteration of the 4D atlas to improve its third and final iteration is a novel technique to approach convergence of the cubic spline fit in four dimensions. To capture variation in mouse development better, more mouse embryo images can be added to the nominal set of 48 mouse embryos, with multiple iterations of re-timestamping also performed.
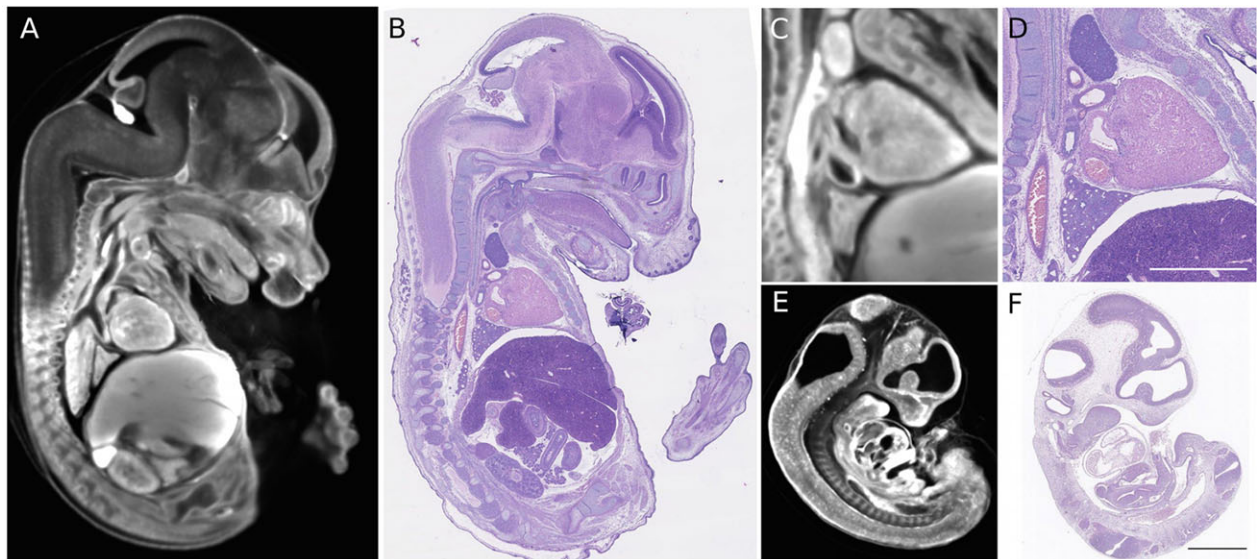
Fig. 8. Use of the 4D atlas to stage Hematoxylin and Eosin histological sections. (A-D) By visual comparison, a comparable section (A) can be found in the 4D atlas for an approximately mid sagittal slice of nominal age E14 (B) by scanning over slice position, slice orientation and embryo age. Details from the images in A and B are shown in C and D, respectively. Identification of the corresponding 4D atlas slice enables identification of the age as E14.05. (E,F) Another example with a younger embryo of nominal age ~E11 that corresponds to E11.50 in the 4D atlas. Scale bar: 1 mm.

This development of an embryonic 4D atlas shares several ideas with a study by Szulc et al., which used *in vivo* 3D magnetic resonance imaging and image registration to describe the anatomical development of postnatal mouse brain (Szulc et al., 2015).

Limitations and future extension of the 4D atlas

The 4D developmental atlas presented here is currently limited in its gestational age range (E11.5-E14.0), which obviously falls well short of the 19 days of gestation in the C57BL/6 mouse. However, this narrow embryonic age range was chosen for several reasons. First, we wanted to test the feasibility of registering images of mouse embryos between two time points in development at 0.5 dpc intervals. Also, OPT images of mouse embryos older than E14.0 are poor in quality because the excitation and emission light are absorbed by the tissue, which becomes opaque at these time points. E11.5 was chosen as the lower bounds of the presented 4D atlas because organogenesis and morphological development occur much faster at dpc earlier than this time point. If anatomical homology is weak or absent between the time points, then image registration fails and the 4D atlas would be poorly constructed. With the success demonstrated by this study, we are confident that earlier mouse embryo development could be captured in the same way, but the time interval between the time points would need to be much smaller. Using somite number or the limb morphometric system instead of gestational days would be better for binning the original data sets for image registration and subsequent cubic spline fitting at earlier time points (E8.0-E11.5). Extending the 4D atlas into late gestation would require another imaging modality. Micro-computed tomography (CT) imaging has been successful in capturing 3D anatomy, both external and internal including a variety of soft, non-mineralized tissues, of late gestation mouse embryos that are stained with iodine (Degenhardt et al., 2010; Metscher, 2009a,b; Wong et al., 2012). A micro-CT late gestation 4D atlas would be much easier to generate because morphological differences in organs during late gestation are mostly due to growth. This would require fewer time points for embryo harvesting and imaging. The OPT and micro-CT 4D atlases then could be merged at the E13.5 or E14.0 time point to build a 4D atlas that was continuous throughout

gestation. Although the fusion of OPT and micro-CT 4D atlases would not be trivial owing to differences in signal intensity and contrast, this challenge could be surmounted using mutual information (Pluim et al., 2003) instead of normalized cross correlation as the similarity measure for image registration as was employed in this study.

Another point of discussion is that the 4D developmental atlas is not representative of absolute time. For example, if the precise conception time of a given embryo was known, and the embryo was extracted at exactly 12.5 dpc, the OPT image of that embryo would not stage perfectly with the E12.5 image of the 4D atlas. We used time (dpc) as the fourth dimension of our continuous staging system because it is easily interpreted by developmental biologists. The time component of the 4D atlas is dependent on the initial image models, which were the average morphology of eight individual mouse embryos dissected at each of six time points. If a different set of 48 embryos were dissected at the exact same time points, the time component of the resultant 4D atlas would be distributed differently based on the population average images generated from the initial data set. Therefore, the 4D atlas' current staging system is subject to a sampling that is relative in time because it is defined by the mouse embryos in the initial set. As noted above, increasing the number of embryos used by reference models in the 4D atlas would presumably improve the atlas' stage calibration in absolute time and also allow estimates of variation.

The current iteration of the 4D atlas staging method complements the previously published limb bud staging method (Boehm et al., 2011) because the atlas method does not accurately stage limb or tail development owing to poor image registration for those structures. This insufficiency is a product of limitations of our image registration algorithm, which does not allow the deformations needed to align structures that are inherently different and variable in their position amongst mouse embryo images, such as the limbs and tail.

Embryonic staging as a phenotyping tool

Previously, we have presented methods to identify where mutant anatomical phenotypes are found in knockout mouse embryo

images (Wong et al., 2012, 2014). Image registration methods were used to localize, in a mutant mouse population, statistical differences in volume, shape, and image intensity. The novel 4D atlas staging system is a first step towards our goal of identifying when in gestational time a mutant phenotype starts to deviate from normal embryonic development in order to understand more deeply, for example, the origins of congenital malformation and disease (birth defects). In particular, embryonic- and perinatal-lethal knockout mouse lines are often growth retarded compared with their wild-type counterparts, but it is often unclear whether growth is uniformly retarded across the whole embryo. The staging system made possible by creating the reference 4D developmental atlas can identify at a fine, precise level growth retardation at the voxel or organ level. The ability to conclude definitively that, for example, the whole mouse embryo is at a given developmental stage but heart growth is retarded by 'X' hours or days post coitum would be highly informative to developmental biologists across a spectrum of subdisciplines.

Precise morphological staging could also add value to phenotyping screens, such as the embryonic lethal pipeline of the International Mouse Phenotyping Consortium (IMPC; www. mousephenotype.org) (Adams et al., 2013), which aims to phenotype all single gene knockout lines in the mouse genome that are embryonic or perinatal lethal in an effort to elucidate gene function. The IMPC is already using both OPT and micro-CT imaging as their primary screens for embryonic lethals, and it has incorporated our previously described method to localize mutant phenotypes into their pipeline (Wong et al., 2014). The addition of a 4D atlas staging system to the IMPC pipeline could help inform when in embryonic development a knocked-out gene of interest is essential to the morphogenesis of a particular organ system.

In conclusion, the 4D atlas staging system presented here has the potential to be the first computer-automated method to identify deviations in morphology over the course of mouse embryo development at the global, structural and voxel levels.

MATERIALS AND METHODS
Sample preparation
For this study, C57BL/6 mice were mated and vaginal plugs detected the following day at noon were defined as 0.5 dpc. Embryos from three litters were harvested at six gestational time points separated by 12-h intervals (E11.5, E12.0, E12.5, E13.0, E13.5 and E14.0). From the three litters, eight mouse embryos were randomly selected as a nominal set of forty-eight embryos. An additional E12.5 C57BL/6 mouse embryo was dissected as an example embryo staged using our 4D atlas. After dissection, embryos were fixed in 4% paraformaldehyde overnight, then transferred to PBS and stored until OPT scanning. Immediately before scanning, embryos were embedded in low melting point agarose, dehydrated through a methanol series, and cleared with BABB, an index of refraction matching solution consisting of a 1:2 benzyl alcohol: benzyl benzoate mixture.

Optical projection tomography imaging
Each mouse embryo was imaged using a previously described custom-built OPT system (Boehm et al., 2011; Wong et al., 2013). Each embryo at the same developmental age (dpc) was acquired at the same microscope magnification and effective pixel size. The overall magnification was adjusted per time point to maximize the detector field-of-view and morphological information collected. Emission autofluorescence OPT was used to acquire 3D images of general morphology over the whole embryo volume (excitation filter: 425/30 nm bandpass; emission filter: 473 nm long-pass). All 48 mouse embryo OPT images were resampled, using cubic interpolation, to an isotropic voxel size of 18 μm^3 to maintain resolution consistency and reduce computational processing time.

Image registration
Group-wise registration: generation of image models
Group-wise image registration was performed as previously described (Boehm et al., 2011; Kovacevic, 2004; Wong et al., 2012, 2014). Briefly, each mouse embryo image was subjected to a six-parameter, rigid registration (three translations, three rotations) towards a model embryo such that every image was identically oriented and positioned in 3D image space. Additionally, a 12-parameter (three translations, three rotations, three scales and three shears) pair-wise affine registration ($N{\times}N{-}1$ registrations) normalized for embryo size and skew. The average of the seven transforms for each mouse embryo image was calculated and applied to that same image. A final population average image was generated from the images resulting from the affine registration. Next, a six-generation multi-scale non-linear registration algorithm was applied (Collins and Evans, 1997; Sharpe et al., 2002; Wong et al., 2013). The scale size at each iteration was: 300 μm, 300 μm, 150 μm, 90 μm, 50 μm and 30 μm. The full-width-half-maximum of the Gaussian blur kernel for each iteration was: 600 μm, 400 μm, 150 μm, 90 μm, 50 μm, and 30 μm. For the first non-linear iteration, each embryo image was registered towards the population average of the affine registration. For subsequent non-linear iterations, each image was registered towards the population average image of the previous non-linear registration iteration.

Source-to-target registration: generation of displacement vectors fields
Source-to-target image registrations were conducted between image models in the direction of increasing developmental time. The resulting displacement vectors for each point in anatomy described its 3D trajectory over gestational time. Source-to-target image registration was performed in the same manner as group-wise registration; however, instead of registering the source images towards a population average image for the affine and non-linear registrations, the mouse embryo images were registered 100% towards the target image.

Similarity measure: normalized cross correlation
Notably, we used an intensity-based image registration, and the similarity measure chosen to maximize the objective function during image registration was normalized cross correlation (Eqn 1). Normalized cross correlation is computed over all voxel positions over a defined discrete grid ($x\varepsilon\Omega$). The optimal value for normalized cross correlation ($X_c{=}1$) would be computed if an image was registered to itself using an identity transformation. Alternatively, the normalized cross correlation coefficient is optimized once the source image (I_S) comes into alignment with the target image (I_T).

$$X_c(I_S, I_T) = \frac{\sum_{x\epsilon\Omega} I_S(x)I_T(x)}{\sqrt{\sum_{x\epsilon\Omega} I_S(x)^2 \sum_{x\epsilon\Omega} I_T(x)^2}} \qquad (1)$$

Author contributions
M.D.W. prepared the mouse embryos for imaging, acquired the image data sets, optimized the image registration, generated the 4D atlas, developed the staging system and wrote the manuscript. M.D.W. and R.M.H. designed the experiments. R.M.H. supervised the study and edited the manuscript. M.C.v.E. helped optimize the image registration. S.S. performed correlations with histology. S.J. performed the segmentations. J.P.L. consulted on image registration and statistical analysis and edited the manuscript. J.C.B. consulted on the developmental staging, provided data sets and edited the manuscript.

Research Chair in Imaging Technologies in Human Diseases and Preclinical Models.

Supplementary information

Supplementary information available online at
http://dev.biologists.org/lookup/suppl/doi:10.1242/dev.125872/-/DC1

References

Adams, D., Baldock, R., Bhattacharya, S., Copp, A. J., Dickinson, M., Greene, N. D. E., Henkelman, M., Justice, M., Mohun, T., Murray, S. A. et al. (2013). Bloomsbury report on mouse embryo phenotyping: recommendations from the IMPC workshop on embryonic lethal screening. *Dis. Model. Mech.* **6**, 571-579.

Boehm, B., Rautschka, M., Quintana, L., Raspopovic, J., Jan, Z. and Sharpe, J. (2011). A landmark-free morphometric staging system for the mouse limb bud. *Development* **138**, 1227-1234.

Collins, D. L. and Evans, A. C. (1997). Animal: validation and applications of nonlinear registration-based segmentation. *Int. J. Pattern Recogn. Artif. Intell.* **11**, 1271-1294.

Degenhardt, K., Wright, A. C., Horng, D., Padmanabhan, A. and Epstein, J. A. (2010). Rapid 3D phenotyping of cardiovascular development in mouse embryos by micro-CT with iodine staining. *Circulation* **3**, 314-322.

Kovacevic, N. (2004). A Three-dimensional MRI Atlas of the Mouse Brain with Estimates of the Average and Variability. *Cereb. Cortex* **15**, 639-645.

Metscher, B. D. (2009a). MicroCT for comparative morphology: simple staining methods allow high-contrast 3D imaging of diverse non-mineralized animal tissues. *BMC Physiol.* **9**, 11.

Metscher, B. D. (2009b). MicroCT for developmental biology: a versatile tool for high-contrast 3D imaging at histological resolutions. *Dev. Dyn.* **238**, 632-640.

Michos, O., Panman, L., Vintersten, K., Beier, K., Zeller, R. and Zuniga, A. (2004). Gremlin-mediated BMP antagonism induces the epithelial-mesenchymal feedback signaling controlling metanephric kidney and limb organogenesis. *Development* **131**, 3401-3410.

Pang, S. C., Janzen-Pang, J., Yat Tse, M., Croy, A. and Tse, D. (2014). *Implant Site Dissections. The Guide to Investigation of Mouse Pregnancy*, pp. 21-42. London: Elsevier Inc.

Papaioannou, V. E. and Behringer, R. R. (2005). *Mouse Phenotypes: A Handbook of Mutation Analysis*, Vol. 5.2, pp. 78.

Pluim, J. P. W., Maintz, J. B. A. and Viergever, M. A. (2003). Mutual-information-based registration of medical images: a survey. *IEEE Trans. Med. Imaging* **22**, 986-1004.

Sharpe, J., Ahlgren, U., Perry, P., Hill, B., Ross, A., Hecksher-Sørensen, J., Baldock, R. and Davidson, D. (2002). Optical projection tomography as a tool for 3D microscopy and gene expression studies. *Science* **296**, 541-545.

Szulc, K. U., Lerch, J. P., Nieman, B. J., Bartelle, B. B., Friedel, M., Suero-Abreu, G. A., Watson, C., Joyner, A. L. and Turnbull, D. H. (2015). 4D MEMRI atlas of neonatal FVB/N mouse brain development. *Neuroimage* **118**, 49-62.

Theiler, K. (1972). *The House Mouse. Development and Normal Stages from Fertilization to 4 weeks of Age. Teratology*, pp. 248-249. New York: Springer.

Walls, J. R., Coultas, L., Rossant, J. and Henkelman, R. M. (2008). Three-dimensional analysis of vascular development in the mouse embryo. *PLoS ONE* **3**, e2853.

Wong, M. D., Dorr, A. E., Walls, J. R., Lerch, J. P. and Henkelman, R. M. (2012). A novel 3D mouse embryo atlas based on micro-CT. *Development* **139**, 3248-3256.

Wong, M. D., Dazai, J., Walls, J. R., Gale, N. W. and Henkelman, R. M. (2013). Design and implementation of a custom built optical projection tomography system. *PLoS ONE* **8**, e73491.

Wong, M. D., Maezawa, Y., Lerch, J. P. and Henkelman, R. M. (2014). Automated pipeline for anatomical phenotyping of mouse embryos using micro-CT. *Development* **141**, 2533-2541.

DEVELOPMENT